Statistical Testing and Material Model Characterization of Aluminum and Titanium for Transport Airplane Rotor Burst Fragment Shielding

August 2007

Final Report

U.S. Department of Transportation
Federal Aviation Administration

NOTICE

This document is disseminated under the sponsorship of the U.S. Department of Transportation in the interest of information exchange. The United States Government assumes no liability for the contents or use thereof. The United States Government does not endorse products or manufacturers. Trade or manufacturer's names appear herein solely because they are considered essential to the objective of this report. This document does not constitute FAA certification policy. Consult your local FAA aircraft certification office as to its use.

This report is available at the Federal Aviation Administration William J. Hughes Technical Center's Full-Text Technical Reports page: actlibrary.tc.faa.gov in Adobe Acrobat portable document format (PDF).

1. Report No. DOT/FAA/AR-07/26	2. Government Accession No.	3. Recipient's Catalog No.

4. Title and Subtitle STATISTICAL TESTING AND MATERIAL MODEL CHARACTERIZATION OF ALUMINUM AND TITANIUM FOR TRANSPORT AIRPLANE ROTOR BURST FRAGMENT SHIELDING		5. Report Date August 2007
		6. Performing Organization Code

7. Author(s) Gregory Kay, Dana Goto, and Richard Couch	8. Performing Organization Report No.

9. Performing Organization Name and Address Lawrence Livermore National Laboratory P.O. Box 808 Livermore, CA 94551	10. Work Unit No. (TRAIS)
	11. Contract or Grant No.

12. Sponsoring Agency Name and Address U.S. Department of Transportation Federal Aviation Administration Air Traffic Organization Operations Planning Office of Aviation Research and Development Washington, DC 20591	13. Type of Report and Period Covered Final Report
	14. Sponsoring Agency Code ANM-100

15. Supplementary Notes

The Federal Aviation Administration Airport and Aircraft Safety R&D Division COTR was Donald Altobelli.

16. Abstract

A previous Lawrence Livermore National Laboratory study focused on experimental measurements that could be used to derive material model representations of aluminum alloy 2024-T3 and the titanium alloy Ti-6Al-4V for use in ballistic impact simulations. The measurements included tensile and compression Hopkinson Bar stress-strain curves and ballistic limit data from gun experiments. The Johnson-Cook model was selected as a means to provide a general-purpose description of material constitutive response and fracture. The results of that project suggested that, for a given material, there might be difficulty in applying a single set of Johnson-Cook parameters to the predictions of penetration through plates of significantly different thicknesses. The present project was designed to explore the suspected "thickness effect" and to establish greater validity for the Johnson-Cook parameterization. Activities again included both Hopkinson Bar and ballistic tests.

The data obtained indicated that the constitutive parameters obtained for the Johnson-Cook model from the previous study are valid for plate material in the range of thicknesses evaluated. The Johnson-Cook failure parameters are not sensitive to this data. The current data also confirmed the anisotropic response of the titanium plate materials and the isotropic response of the aluminum plate material. The Johnson-Cook failure parameters were recalibrated in an attempt to attain consistency between simulations and the available ballistic limit measurements. The Johnson-Cook failure algorithm, as currently implemented, did not do an adequate job in determining the type of target failure for the target thicknesses and material considered in this study (aluminum 2024-T3/T351). This is especially important as petaling failure modes tend to absorb less energy than the shear localization failure modes. However, the Johnson-Cook failure algorithm does appear to be able to do an adequate job when the range of target thicknesses is restricted.

17. Key Words Ballistics, Projectile, Plugging (shear failure), Petaling, Aluminum ballistic limit, Fragment simulant projectile	18. Distribution Statement This document is available to the U.S. public through the National Technical Information Service (NTIS), Springfield, Virginia 22161.		
19. Security Classification. (of this report) Unclassified	20. Security Classification. (of this page) Unclassified	21. No. of Pages 26	22. Price

Form DOT F 1700.7 (8-72)   Reproduction of completed page authorized

ACKNOWLEDGEMENT

TABLE OF CONTENTS

Page

LIST OF FIGURES

LIST OF TABLES

LIST OF ACRONYMS

Al	Aluminum
LLNL	Lawrence Livermore National Laboratory
UCB	University of California at Berkeley
FSP	Fragment simulant projectile
Ti	Titanium

EXECUTIVE SUMMARY

A previous Lawrence Livermore National Laboratory study focused on experimental measurements that could be used to derive material model representations of aluminum alloy 2024-T3 and the titanium alloy Ti-6Al-4V for use in ballistic impact simulations. The measurements included tensile and compression Hopkinson Bar stress-strain curves and ballistic limit data from gun experiments. The Johnson-Cook model was selected as a means to provide a general-purpose description of material constitutive response and fracture. The results of that project suggested that, for a given material, there might be difficulty in applying a single set of Johnson-Cook parameters to the predictions of penetration through plates of significantly different thicknesses. The present project was designed to explore the suspected "thickness effect" and to establish greater validity for the Johnson-Cook parameterization. Activities again included both Hopkinson Bar and ballistic tests.

The data obtained indicated that the constitutive parameters obtained for the Johnson-Cook model from the previous study are valid for plate material in the range of thicknesses evaluated. The Johnson-Cook failure parameters are not sensitive to this data. The current data also confirmed the anisotropic response of the titanium plate materials and the isotropic response of the aluminum plate material.

The Johnson-Cook failure parameters were recalibrated in an attempt to attain consistency between simulations and the available ballistic limit measurements. The Johnson-Cook failure algorithm, as currently implemented, did not do an adequate job in determining the type of target failure for the target thicknesses and material considered in this study (aluminum 2024-T3/T-351). This is especially important as petaling failure modes tend to absorb less energy than the shear localization failure modes. However, the Johnson-Cook failure algorithm does appear to be able to do an adequate job when the range of target thicknesses is restricted.

1. INTRODUCTION.

A previous Lawrence Livermore National Laboratory (LLNL) study [1 and 2] focused on experimental measurements that could be used to derive material model representations of aluminum (Al) alloy 2024-T3 and the titanium (Ti) alloy Ti-6Al-4V for use in ballistic impact simulations. The measurements included tensile and compression Hopkinson Bar stress-strain curves and ballistic limit data from gun experiments. The Johnson-Cook model was selected as a means to provide a general-purpose description of material constitutive response and fracture. The results of that project suggested that, for a given material, there might be difficulty in applying a single set of Johnson-Cook parameters to the predictions of penetration through plates of significantly different thicknesses.

This project was designed to explore the suspected "thickness effect" and to try to establish greater validity for the Johnson-Cook parameterization. Activities again included both Hopkinson Bar and ballistic tests. The purpose of the Hopkinson Bar measurements was to obtain stress-strain measurements from thicker plates than used in the previous study [1 and 2] and observe any differences in constitutive response due to thickness. Aluminum plates of 0.5″ thickness were used in this study in comparison to 0.15″ thick plates previously. The Ti measurements were made with 0.75″ plates in comparison to 0.25″ from the previous effort. Both tension and compression data were taken.

It was planned that the ballistic tests would provide ballistic limit data on 0.5″ Al and 0.75″ Ti plates. Flat-nosed cylindrical steel projectiles were used. Data was obtained on Al. There were experimental problems associated with the 0.75″ Ti plates. When the Al data became available and were compared with the data being obtained at University of California at Berkeley (UCB), it was decided to focus resources on the analysis of the two data sets. The Ti experiments were eliminated from this study.

The analysis performed by LLNL was focused on determining the validity of the Johnson-Cook parameters available from the previous study [1 and 2] and updating them if necessary. A major, and not totally resolved, issue was the separation of general code dependencies from material model dependencies in interpreting numerical simulations of the experiments. A recalibration of the Johnson-Cook failure parameters was done in an attempt to attain consistency with all the data available.

2. EXPERIMENTAL RESULTS.

2.1 HOPKINSON BAR MEASUREMENTS.

The Al 2024-T351 was purchased as 0.5″ plate material under specification Aerospace Material Specification (AMS) 4037_Rev-M. Sufficient material was purchased for both Hopkinson Bar and ballistic tests. The Ti 6Al-4V material was from 0.75″ plate material provided by Pratt & Whitney during the previous program [2]. The tension and compression data for the Al are shown in figures 1 and 2. The corresponding data for the Ti are provided in figures 3 and 4. Tables 1 and 2 summarize the Hopkinson Bar test data for both the Al and Ti tested.
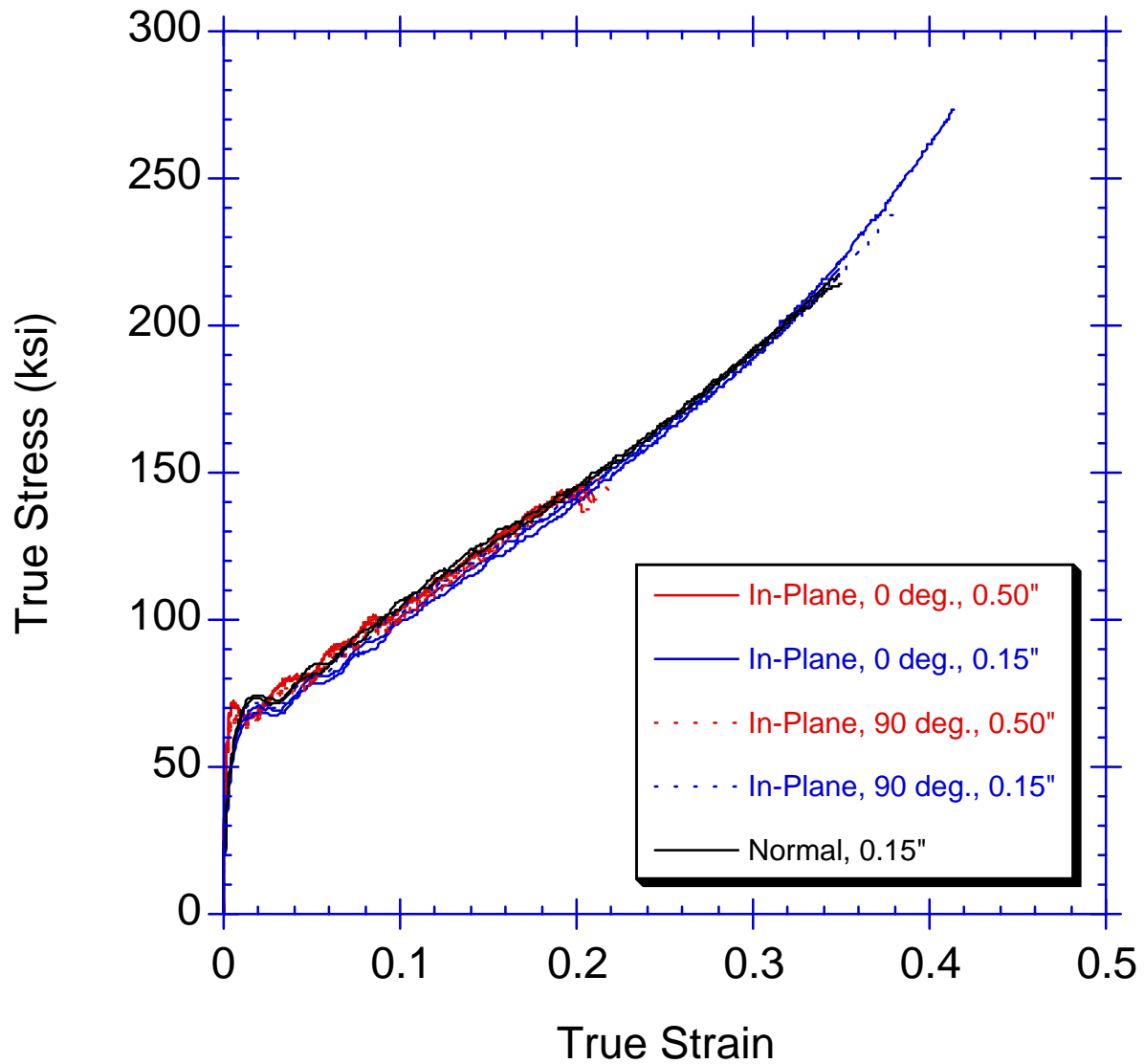
Figure 1. Hopkinson Bar Dynamic Compression Data for Al 2024-T351
(Note: The current data at 0.5″ is consistent with the earlier data for the thinner plate. There is no indication of asymmetry in the material response.)
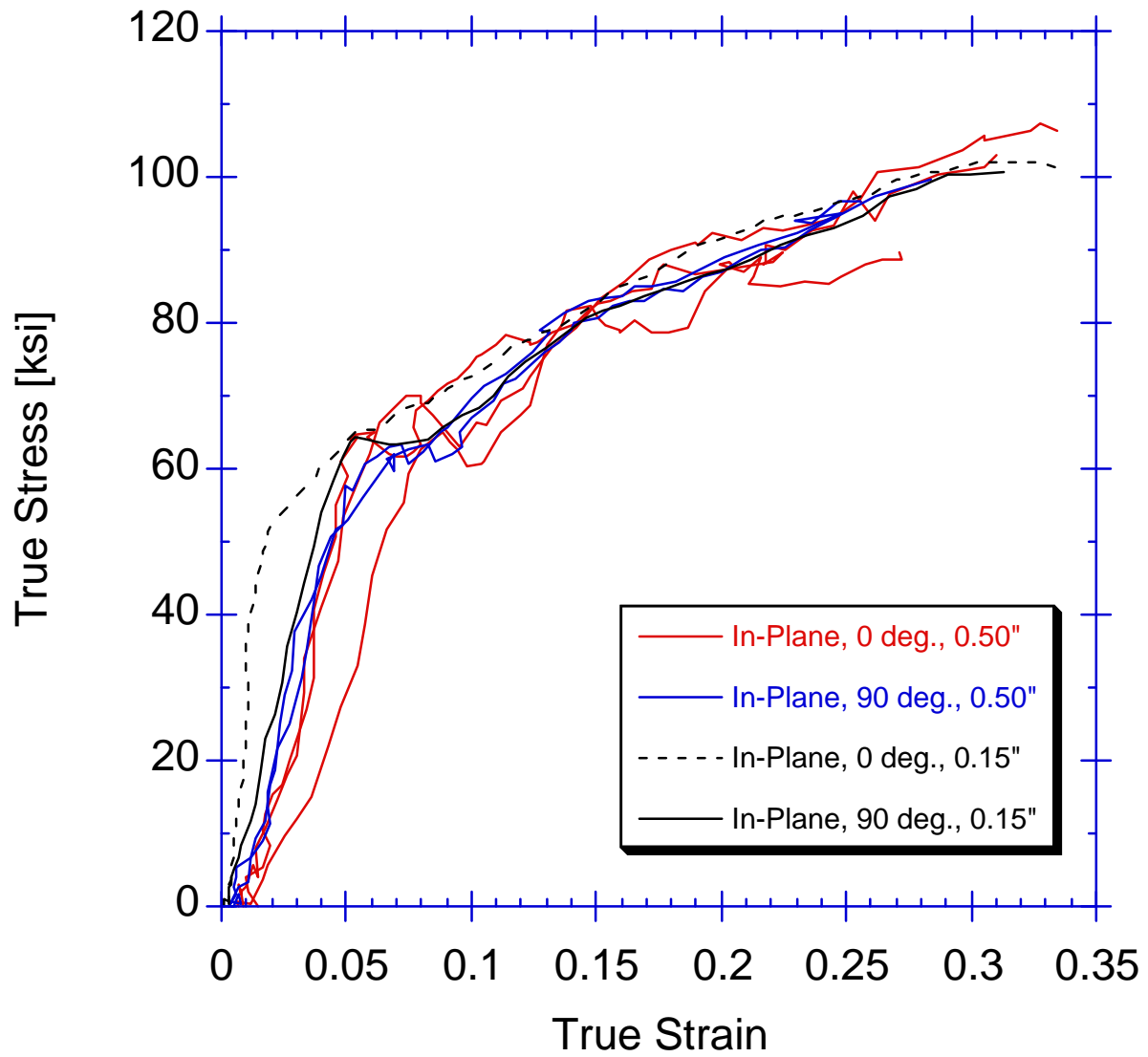
Figure 2. Hopkinson Bar Dynamic Tension Data for Al 2024-T351
(Note: The results for the two plate thicknesses are consistent and there is no indication of asymmetry in response.)

Figure 3. Hopkinson Bar Dynamic Compression Data for the Ti 6AL-4V
(Note: The data for the two plate thicknesses are consistent. The asymmetry previously
observed [2] is reproduced in the current measurements.)
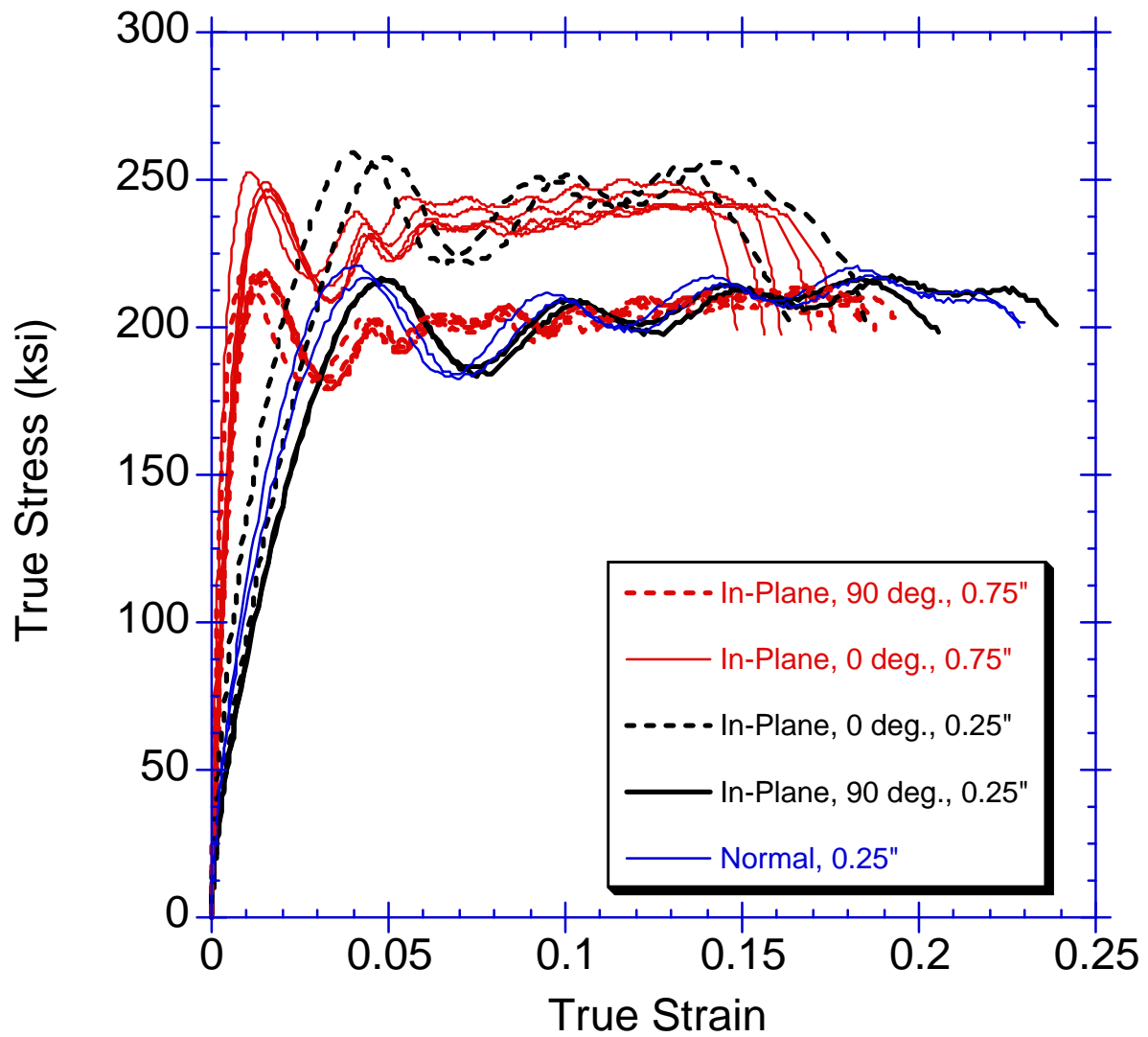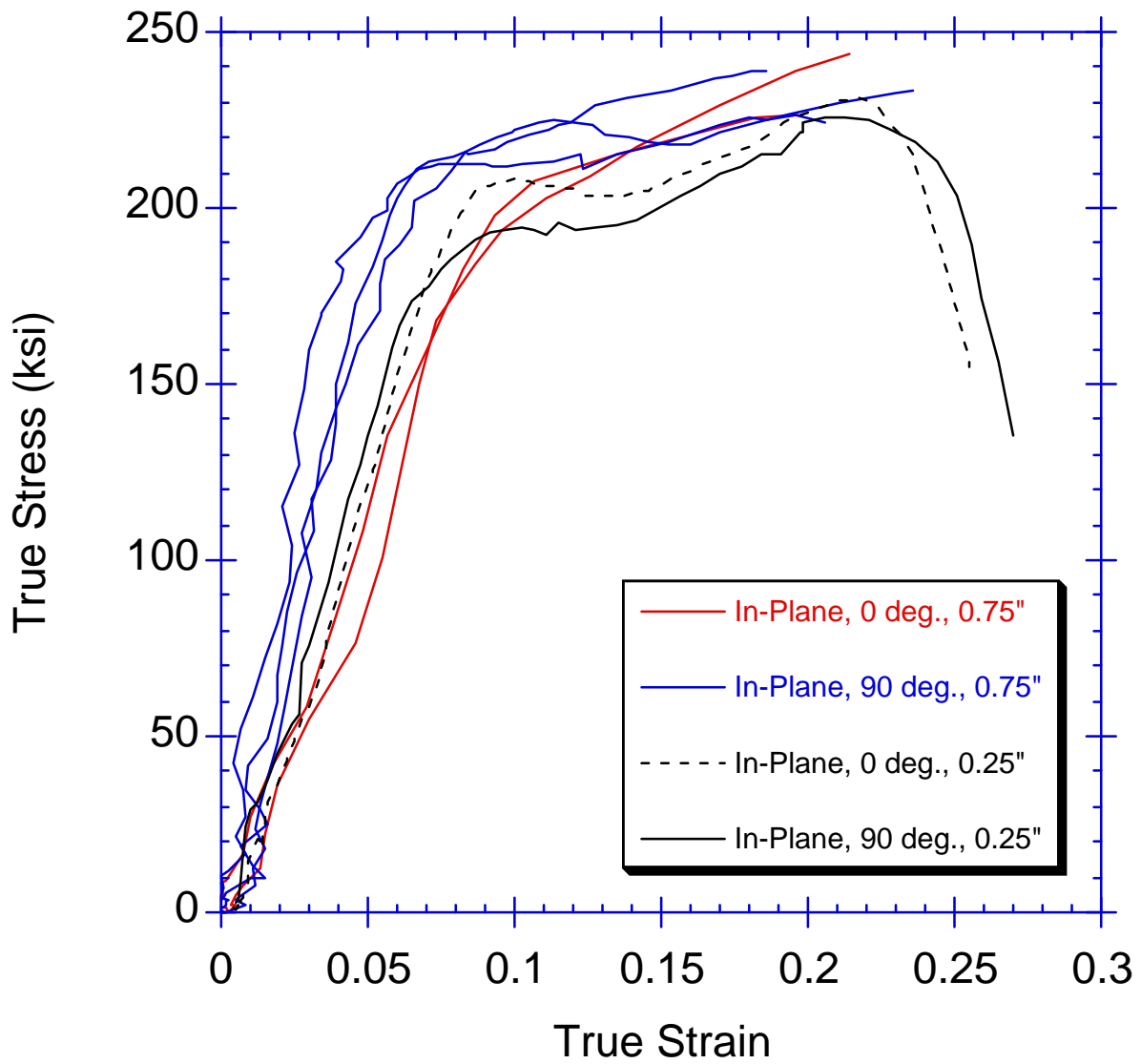
Figure 4. Hopkinson Bar Dynamic Tension Data for the Ti 6AL-4V
(Note: The data for the two plate thicknesses are similar but not precisely consistent. The asymmetry observed in the compression data is more apparent in the current measurements than in the limited data set available from the previous study [2].)

Table 1. Summary of Hopkinson Bar Compression Tests

Specimen ID	Initial Average Height (inch)	Initial Average Diameter (inch)	Posttest Height (inch)	Posttest Minimum Diameter (inch)	Posttest Maximum Diameter (inch)	Strain Rate (sec^{-1}) Based on True Strain
Al-1 (0 deg.)	0.2005	0.1997	0.141	0.235	0.246	exp. problem
Al-2 (0 deg.)	0.2001	0.2004	0.138	0.237	0.249	exp. problem
Al-3 (0 deg.)	0.2003	0.2003	0.138	0.237	0.249	3200
Al-4 (0 deg.)	0.2004	0.2003	0.140	0.235	0.247	3200
Al-5 (0 deg.)	0.2004	0.1999	0.137	0.238	0.249	3200
Al-6 (90 deg.)	0.2004	0.2001	0.139	0.236	0.248	3100
Al-7 (90 deg.)	0.2003	0.1998	0.140	0.234	0.248	3100
Al-8 (90 deg.)	0.2004	0.1999	0.139	0.235	0.247	3100
Al-9 (90 deg.)	0.2004	0.2003	0.134	0.240	0.253	3400
Al-10 (90 deg.)	0.2004	0.2002	0.137	0.237	0.250	3200
Ti-1 (0 deg.)	0.2004	0.2007	0.166	0.210	0.230	2400
Ti-2 (0 deg.)	0.2003	0.2008	0.168	0.211	0.228	2300
Ti-3 (0 deg.)	0.1997	0.2007	0.168	0.212	0.226	2300
Ti-4 (0 deg.)	0.2004	0.2007	0.168	0.208	0.230	2300
Ti-5 (0 deg.)	0.2004	0.2006	0.170	0.211	0.225	2200
Ti-6 (90 deg.)	0.2004	0.2007	0.175	0.211	0.221	2000
Ti-7 (90 deg.)	0.2003	0.2007	0.171	0.215	0.220	2100
Ti-8 (90 deg.)	0.2000	0.2007	broken	broken	broken	1900
Ti-9 (90 deg.)	0.2005	0.2007	0.175	0.212	0.218	1900
Ti-10 (90 deg.)	0.2000	0.2007	0.172	0.214	0.219	2000

Table 2. Summary of Hopkinson Bar Tension Tests

Specimen	Elongation (%)	Specimen	Elongation (%)
Ti-1 0 deg.	17.8	Al-1 0 deg.	29.5
Ti-4 0 deg.	15.3	Al-2 0 deg.	28.5
Ti-5 0 deg.	14.5	Al-3 0 deg.	27.0
Ti-1 90 deg.	18.4	Al-4 90 deg.	26.2
Ti-2 90 deg.	13.4	Al-5 90 deg.	25.6
Ti-5 90 deg.	14.8	Al-6 90 deg.	26.0

Strain rates were in the range 5000-7000 sec^{-1}

The data obtained indicated that the constitutive parameters obtained for the Johnson-Cook model from the previous study [2] are valid for plate material in the range of thicknesses evaluated. The Johnson-Cook failure parameters are not sensitive to this data. The current data also confirmed the anisotropic response of the Ti plate materials and the isotropic response of the Al plate material.

The projectiles were 0.5″ diameter and 1.0″ long cylinders made of tool steel with a Rockwell C hardness of 44. The targets were 6″ x 6″ Al 2024 T-351 plates of 0.5″ thickness. The impact velocities were measured by determining the time interval between two interrupted laser beams. Shots (c) and (d) of figure 5 were interpreted as being an indication of the uncertainty in material response. The ballistic limit velocity of 869 ft/sec was obtained by averaging the impact velocity of those two shots. Table 3 is a summary of the ballistic test results.
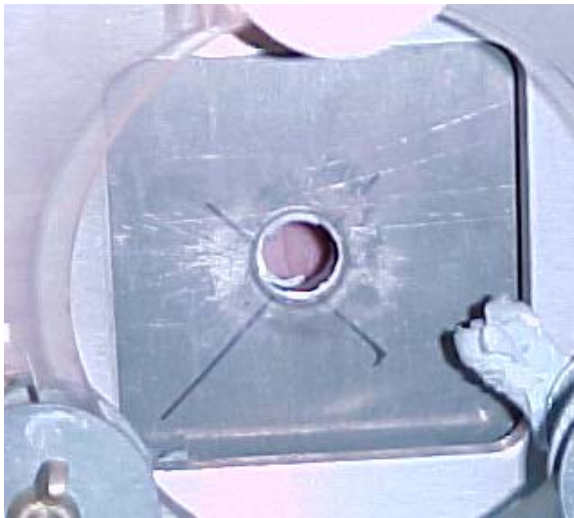
(a) velocity = 919 ft/sec; hole created

(b) velocity = 840 ft/sec; bulge, no crack

(c) velocity = 873 ft/sec; bulge, cracking

(d) velocity = 866 ft/sec; hole created

Figure 5. Summary of the Tests Used to Determine the Ballistic Limit
(Steel cylinders of diameter 0.5″ and length 1.0″ impacted 0.5″ Al 2024-T351 plates.)

Table 3. Summary of Ballistic Tests

Shot	Velocity (ft/sec)	Result
a	919	hole
b	840	bulge, no crack
c	873	bulge, cracking
d	866	hole

The ballistic limit was deduced to be 869 ft/sec.

3. MATERIAL MODEL CHARACTERIZATION RESULTS.

3.1 INTRODUCTION.

This section of the report describes the determination of Johnson-Cook failure parameters for Al 2024-T3/351. A previous LLNL report [1] described the determination and validation of Johnson-Cook failure parameters for Al 2024-T3 that was based on ballistic limit testing of 0.100″ and 0.150″ Al 2024-T3 sheets. The projectiles in those tests were Ti fragment simulant projectile (FSP) cylinders. The FSP is a 0.050″ diameter cylinder with a beveled nose [3].

Overly soft (wider range than desired) ballistic limit predictions were obtained when these parameters were used to simulate the tests of 0.5″ steel spheres impacting 0.125″ thick Al 2024-T3 plates. This predictive inadequacy initiated an effort to enhance predictive capability by expanding and changing the database for determining the Johnson-Cook failure parameters. The new database contained results from UCB tests of 0.5″ diameter spherical steel projectiles impacting Al 2024-T3 target sheets of 0.0625″ and 0.125″ thicknesses and Al 2024-T351 target plate of 0.250″ thickness [4]. Data obtained from FSP impacts into Al 2024-T3 0.150″ target plates and 0.5″ diameter spherical and 0.5″ diameter cylindrical steel projectiles impacting 0.1875″ thick Al 2024-T3 target plates was employed in an attempt to verify the new Johnson-Cook failure parameters. Also, in the verification database, were results from 0.5″ diameter cylinders impacting Al 2024-T351 plates. The failure parameter database is shown in table 4.

Table 4. Al 2024-T3/T351 Data Sets Used in Johnson-Cook Failure Coefficient Determination

Projectile (0.5″ diameter)	Plate Thickness (inch)	Ballistic Limit Data	Post Ballistic Limit Data	Data Originator	Data Set Use
Sphere	0.063 (T-3)	Yes	Yes	UCB	Parameter determination
Sphere	0.125 (T-3)	Yes	Yes	UCB	Parameter determination
Sphere	0.250 (T-351)	Yes	Yes	UCB	Parameter determination
Cylinder	0.500 (T-351)	Yes	No	LLNL	Parameter validation

Table 4. Al 2024-T3/T351 Data Sets Used in Johnson-Cook Failure
Coefficient Determination (Continued)

Projectile (0.5″ diameter)	Plate Thickness (inch)	Ballistic Limit Data	Post Ballistic Limit Data	Data Originator	Data Set Use
FSP	0.150 (T-3)	Yes	No	LLNL	Parameter validation
Sphere	0.1875 (T-3)	Yes	Yes	UCB	Parameter validation
Cylinder	0.1875 (T-3)	Yes	Yes	UCB	Parameter validation

3.2 JOHNSON-COOK FAILURE PARAMETERS.

Failure accumulation in the Johnson-Cook model, more fully described in reference 5, defines the strain at fracture as:

$$\varepsilon_{failure} = \left[D_1 + D_2 \exp(D_3\sigma^*)\right]\left[1 + D_4 \ln(\dot{\varepsilon}^*)\right]\left[1 + D_5 T^*\right] \tag{1}$$

where σ^*, the normalized pressure, is the ratio of the pressure to the effective stress, i.e., $\sigma^* = \dfrac{pressure}{\overline{\sigma}}$.

The nondimensional temperature $T^* = \dfrac{T - T_{room}}{T_{melt} - T_{room}}$ where T is the current temperature, T_{room} is the ambient temperature, and T_{melt} is the melt temperature. Adiabatic conditions are assumed such that all internal plastic work is converted into temperature change, i.e., $\Delta T = \dfrac{\overline{\sigma}\overline{\varepsilon}^p}{\rho C_v}$, where $\overline{\sigma}$ is the effective stress, $\overline{\varepsilon}^p$ is the effective plastic strain, ρ is the mass density, and C_v is the constant volume specific heat. The effective plastic strain $\overline{\varepsilon}^p$ is defined by $\overline{\varepsilon}^p = \int_0^t d\overline{\varepsilon}^p$, where the incremental plastic strain $d\overline{\varepsilon}^p$ is determined from the incremental plastic strain tensor $d\varepsilon_{ij}$, such that $d\overline{\varepsilon}^p = \sqrt{\dfrac{2}{3} d\varepsilon_{ij} d\varepsilon_{ij}}$. The effective stress $\overline{\sigma}$ is defined by $\overline{\sigma} = \sqrt{\dfrac{3}{2} \sigma_{ij} \sigma_{ij}}$. The nondimensional strain rate $\dot{\varepsilon}^*$ is the ratio of the effective plastic strain rate $\dot{\overline{\varepsilon}}^p$ to the reference strain rate $\dot{\varepsilon}^0$ (usually equal to 1.0), i.e., $\dot{\varepsilon}^* = \dfrac{\dot{\overline{\varepsilon}}^p}{\dot{\varepsilon}^0}$.

The first set of brackets in the Johnson-Cook fracture model (equation 1) are intended to represent the observation that the strain to fracture decreases as the hydrostatic tension increases.

9

The second set of brackets in the strain to failure expression represent the effect of an increased strain rate on the material ductility, while the third set of brackets represent the effect of thermal softening on the material ductility. Fracture occurs in the Johnson-Cook model when the damage parameter D exceeds 1.0. The evolution of D is given by the accumulated incremental effective plastic strains divided by the current strain at fracture

$$D = \sum \frac{\Delta \bar{\varepsilon}^{\,p}}{\varepsilon_{failure}}$$

(2)

3.3 RESULTS OF USING THE NEW DATABASE.

Ballistic limits were determined in the simulations by employing a unique set of failure strain parameters to determine target fragment velocities for a range of initial projectile velocities. Initial velocity and residual velocity results were determined for the entire parameter determination database. The failure parameters were then varied until a satisfactory fit to the data was obtained from all the initial velocity and residual velocity simulation sets. Examples of simulations are shown in figures 6 and 7. Figure 6 depicts a 0.5″ sphere impacting a 0.250″ plate at 295 ft/sec. Figure 7 shows the simulated results of the impact of a 0.5″ cylinder and a 0.5″ plate at 295 ft/sec. In these figures, the red regions indicate Johnson-Cook failure parameters of 1.0 (total material failure). Material failure in the spherical impact case started near the bottom surface of the plate and proceeded toward the impact surface of the plate. The tensile stress dominated failure progression was due in part to nonlocal plate bulging from the spherical projectile. The shear failure progression that occurred in the cylindrical impact example was very localized and occurred from the top down.
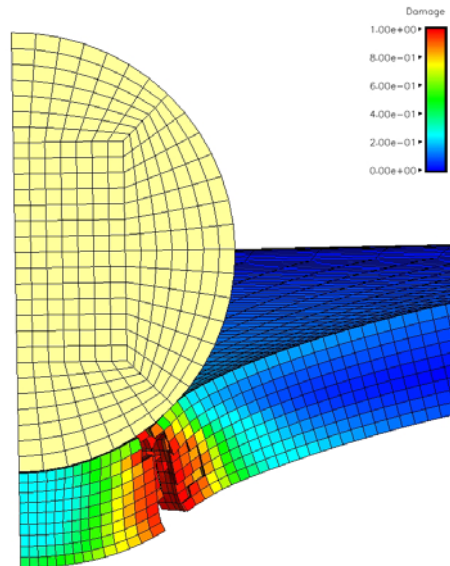

Figure 6. Simulation of a 0.5″ Sphere Impacting a 0.250″ Thick Al 2024-T351 Plate
at 295 ft/sec
(Predicted petaling failure does not compare with observed failure mechanism.)
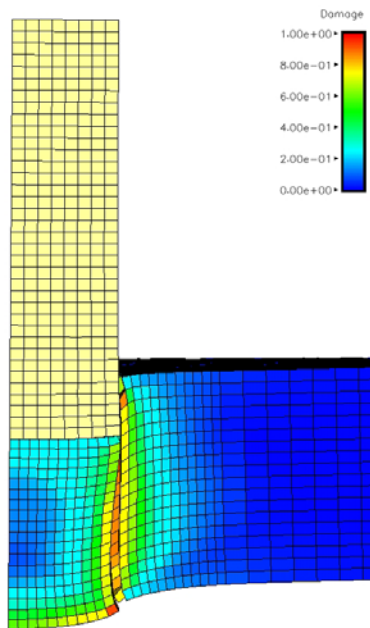
Figure 7. Simulation Results of a 0.5″ Cylinder Impacting a 0.125″ Thick Al 2024-T3 Plate
at 295 ft/sec
(Predicted localized shear failure compares with observed failure.)

A measure of the ability of the Johnson-Cook failure algorithm to differentiate between different stress states that can arise due to differences in target geometries is shown in figure 8. In this figure, the strain at failure (as predicted by the Johnson-Cook model) is plotted as a function of the normalized pressure (the mean stress divided by the effective stress). The Johnson-Cook failure algorithm predicts primarily tensile states of stress (negative normalized pressures) in the local failure regions of the spherical projectiles. This should have led to a petaling type failure for all targets. This was the case for the thinner (0.0625″ and 0.125″) plates, but the 0.250″ target failures included shear localizations as well as some petaling failures. A 0.5″ diameter cylindrical projectile's more shear dominated/compressive state of stress is shown in the positive normalized pressure regions of the curve shown in figure 8.

The chart shows Failure strain (y-axis, 0 to 1) versus Normalized pressure (x-axis, -1.5 to 1.5). Annotations on the chart:

$$\dot{\varepsilon}^* = 5000 \text{ sec}^{-1}$$
$$T^* = 0.1$$

$$\varepsilon_{failure} = \left[D_1 + D_2 \exp(D_3 \sigma^*)\right]\left[1 + D_4 \ln(\dot{\varepsilon}^*)\right]\left[1 - D_5 T^*\right]$$

1.1 JOHNSON-COOK FAILURE STRAIN

Predicted response region for 0.5" spheres and 0.063", 0.125" and 0.250" plates

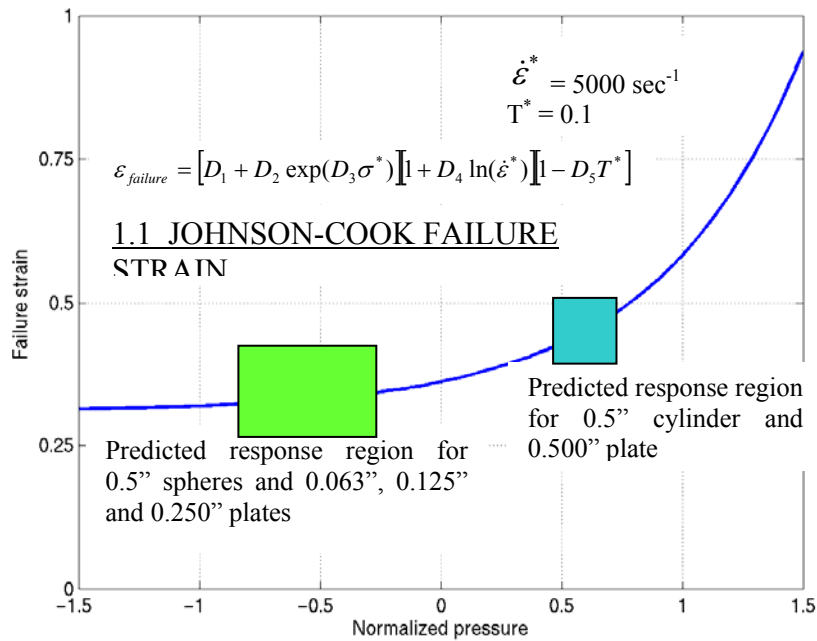Predicted response region for 0.5" cylinder and 0.500" plate

Figure 8. Failure Strain Versus Normalized Pressure as Predicted by the Johnson-Cook Failure Algorithm [3]

Plots of measured and calculated fragment velocities versus initial projectile velocities are shown in figure 9 for the data set that was employed to obtain the best-fit Johnson-Cook failure parameters. The revised Al 2024-T3/T351 flow surface obtained from reference 2 was used in these simulations. The red, green, and blue circles of figure 9 represent individual data from reference 4 for the spherical projectile 0.063″, 0.125″, and 0.250″ plate tests, respectively. The black Xs in figure 9 represent individual simulation results. The simulations predict a slightly higher ballistic limit for the 0.063″ plate, but track the postballistic limit fragment velocities quite well. The 0.125″ plate simulations predict both the ballistic limit and postballistic limit fragment velocities, while the 0.250″ simulations predict a lower than measured ballistic limit. The failure parameters that were used to obtain the results in figure 9 were:

- $D_1 = 0.310$
- $D_2 = 0.045$
- $D_3 = 1.700$
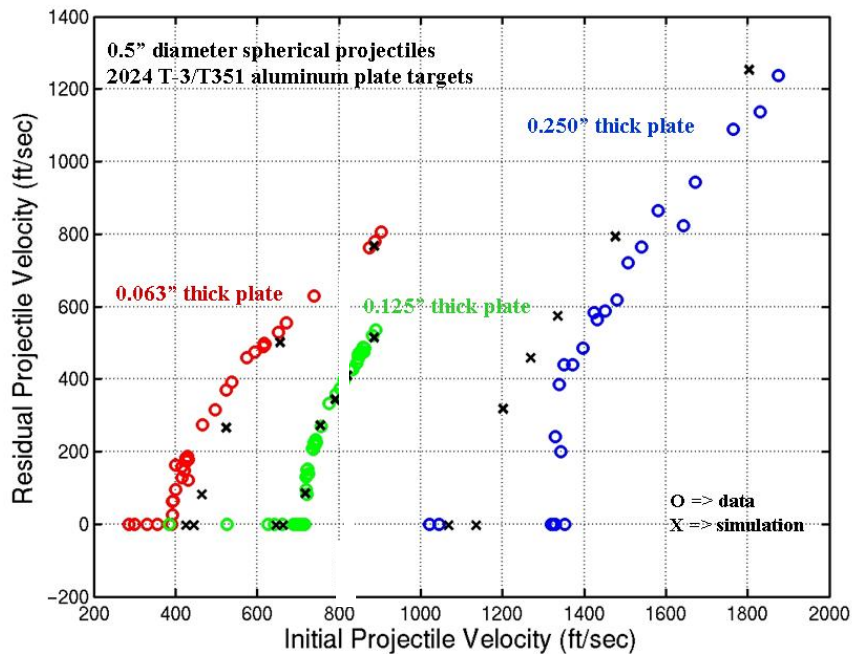- $D_4 = 0.005$
- $D_5 = 0.0$

12

Figure 9. Residual Fragment Velocity Versus Initial Projectile Velocity Using a Single Set of Failure Parameters
(The parameters were determined from this data set.)

Simulations were made of previous FSP tests that were conducted at LLNL [3] and spherical impactor tests at UCB [4] to see how well the revised failure parameters performed against data that was not used in the fitting process. The results are shown in figures 10 and 11. As indicated, for a constant thickness (0.1875″) Al 2024-T3 target, the failure parameters did an adequate job predicting the cylindrical impactor data, but did a poor job predicting the spherical impactor results. The FSP projectile 0.150″ Al target predictions are marginal at best, as they underpredicted the measured ballistic limit. The underprediction of the ballistic limit was even more pronounced for the 0.5″ cylinder projectile impacting 0.500″ Al 2024-T3 target tests from this study (postballistic limit data was not available).
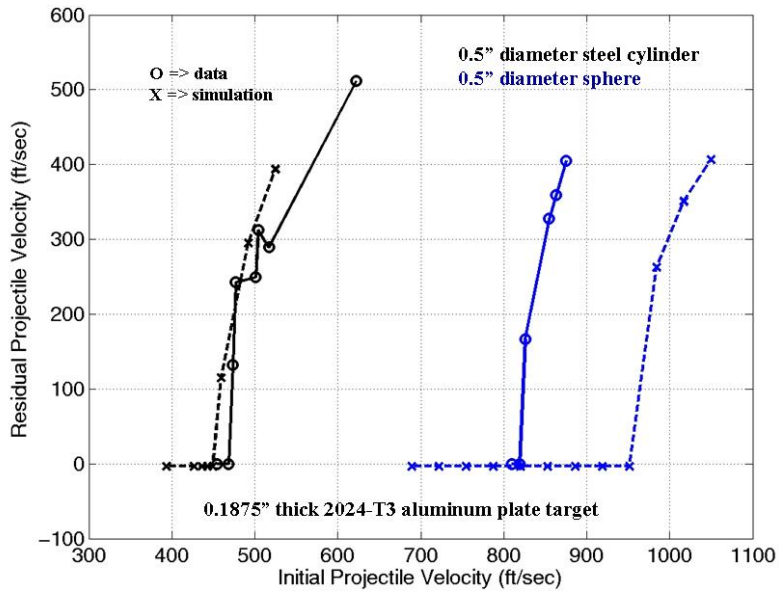
13

Figure 10. Failure Parameter Verification for a 0.1875″ Thick Al 2024-T3 Plate Target
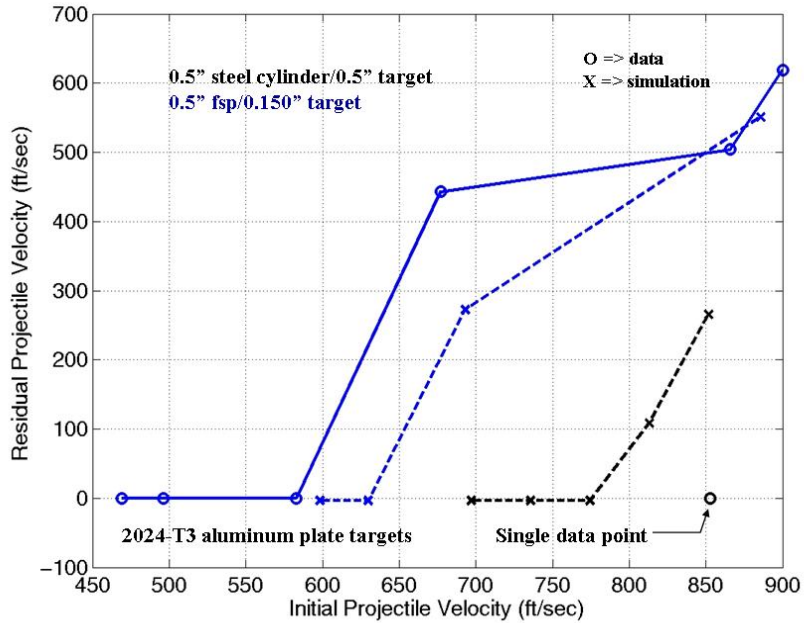(This data was not used in the failure parameter fitting process.)

Figure 11. Failure Parameter Verification Employing Data Not Used in the Parameter
Fitting Process
(This data was not used in the failure parameter fitting process.)

Comparisons of measured and calculated ballistic limit velocities when damage parameters were determined separately for two target thickness ranges are shown in figures 12 and 13. In these figures, the best-fit Johnson-Cook failure parameters were determined for target thicknesses less than 0.25″ and target thickness equal to 0.25″. The revised Al 2024-T3 flow surface obtained from reference 2, was also used in these simulations. The simulation results compare favorably with the data in both figures, tending to support the theory of a Johnson-Cook failure algorithm target thickness dependency.
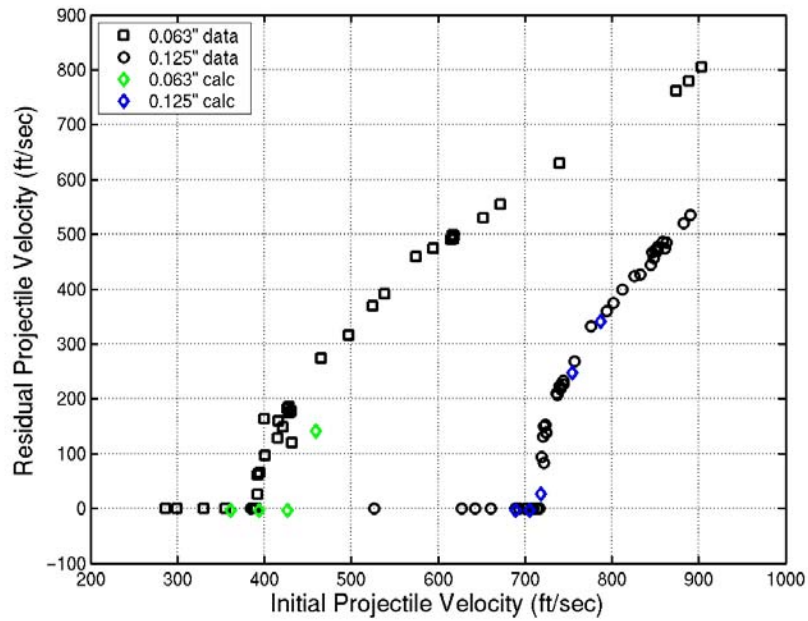

Figure 12. Residual Fragment Velocity Versus Initial Projectile Velocity Using a Specialized Set of Failure Parameters for Al 2024-T3 Target Thicknesses Less Than 0.250″ (Spherical projectiles were 0.5″ in diameter.)
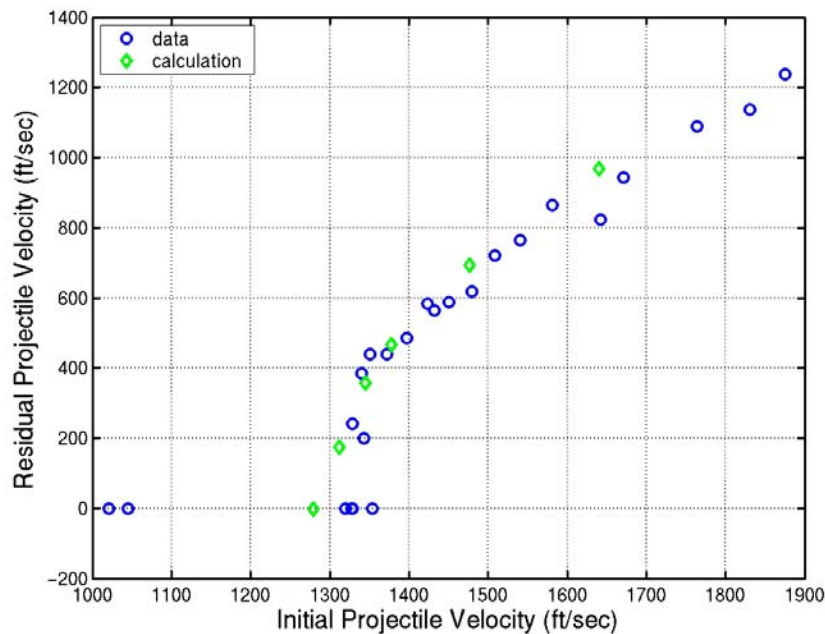
Figure 13. Residual Fragment Velocity Versus Initial Projectile Velocity Using a Specialized
Set of Failure Parameters for an Al 2024-T351 Target Thickness of 0.25″
(Spherical projectiles were 0.5″ in diameter.)

3.4 SUMMARY.

Johnson-Cook failure strain parameters for Al 2024-T3/T351 were developed from a ballistic
limit database that included spherical projectiles and impact plate thicknesses of 0.063″, 0.125″,
and 0.250″. This database produced tensile as well as localized shear modes of failure. The
modified Johnson-Cook failure parameters did a somewhat adequate job of predicting the
measured ballistic limits (the failure parameters were based on the UCB data), but there was a
bias toward underpredicting the thicker plate ballistic limit. The failure parameters did not do an
adequate job when they were employed to predict ballistic limits of other data that was not in the
failure parameter determination database. When the failure parameter determination database
was divided into two separate thickness regions, specialized failure parameters for each thickness
region were able to do an adequate job of predicting ballistic limit results for the data on which
they (the failure parameters) were based. This tends to support the theory of a Johnson-Cook
failure algorithm target thickness dependency.

4. CONCLUSIONS.

The data obtained indicated that the constitutive parameters obtained for the Johnson-Cook
model from the previous study are valid for aluminum 2024-T3/T351 target material in the range
of thicknesses evaluated. The Johnson-Cook failure parameters are not sensitive to this data.
The current data also confirmed the anisotropic response of the titanium plate materials and the
isotropic response of the aluminum plate material.

16

The Johnson-Cook failure algorithm, as currently implemented, did not do an adequate job in determining the type of target failure for the multiple target thicknesses considered in this study (aluminum 2024-T3/T351). This is especially important because petaling failure modes tend to absorb less energy than the shear localization failure modes. However, the Johnson-Cook failure algorithm does appear to be able to do an adequate job when the range of target thicknesses is restricted and the parameters are adjusted to fit a representative test data set.

5. REFERENCES.

1. Kay, Gregory, "Failure Modeling of Titanium 6Al-4V and Aluminum 2024-T3 With the Johnson-Cook Material Model," FAA report DOT/FAA/AR-03/57, September 2003.

2. Lesuer, Donald, "Experimental Investigation of Material Models for T-6Al-4V Titanium and 2024-T3 Aluminum," FAA report DOT/FAA/AR-00/25, September 2000.

3. Gugolowski, R. and Morgan, B., "Ballistic Experiments With Titanium and Aluminum Targets," FAA report DOT/FAA/AR-01-21, April 2001.

4. Kelley, Sean and Johnson, George, "Statistical Testing of Aircraft Materials for Transport Airplane Rotor Burst Fragment Shielding," FAA report DOT/FAA/AR-06/9, May 2006.

5. Johnson, G.R. and Cook, W.H., "Fracture Characteristics of Three Metals Subjected to Various Strain, Strain Rates, Temperatures, and Pressures," *Engineering Fracture Mechanics,* Vol. 21, No. 1, 1985, pp. 31-48.